Blending of cements - influence on porosity and chloride resistance

Andreas Leemann[1], Roman Loser[1], Pavel Trtik[1] and Beat Münch[1]

[1] Empa, Dübendorf, Switzerland

ABSTRACT: Portland cement production accounts for about 5% of the world wide CO_2 emissions. The sustainability of Portland cement systems can be improved when clinker is substituted with mineral admixtures. However, the durability of cementitious materials produced with such blended cements has to be maintained. Mortars with a pure ordinary Portland cement and four blended cements were produced to study the effects of cement substitution on the pore system and the resulting chloride resistance. Both the resulting pore system and its development with time were affected by the substitution of clinker, which directly affected the chloride resistance. The use of limestone powder decreased chloride resistance while the use of slag and fly ash lead to an improvement. However, the beneficial effect of fly ash was not apparent before an age of 182 days was reached.

1 INTRODUCTION

Today the partial substitution of cement clinker with mineral admixtures is mandatory to decrease the CO_2 emissions resulting from Portland cement production (e.g. Gartner, 2004). However, such a substitution is only sustainable, when the durability of mortar and concrete produced with blended cements is not decreased. This applies in particular to the resistance to chlorides, as they are the main cause for damages in reinforced concrete structures worldwide. It must be noticed that depending on the mineral admixtures used, the development of the pore system with time and its characteristics are changed. Due to these changes in the pore system, the chloride resistance is influenced. The addition of slag can lead to an increase in chloride resistance (Niu etal., 2002; Luo et al., 2003; Quellet et al., 2007, Loser et al., 2010). In contrast, the addition of limestone powder to cement can increase porosity and decrease chloride resistance (Tsivilis et al., 1999; Tsivilis et al., 2003; Matschei et al., 2007). In the relation between porosity and permeability, the contact zone between cement paste and aggregate, the so-called interfacial transition zone (ITZ), is supposed to play an important role (Farran, 1956; Winslow et al., 1994; Garbozci & Bentz, 1996; Scrivener & Nemati, 1996). However, quantitative data about the porosity in the ITZ are scarce (Scrivener et al., 1988; Crumbie, 1994; Diamond & Huang, 1998; Leemann et al., 2006).

The goal of this study is to assess the influence of cement blending on chloride resistance and to link the development of the pore system with the development of chloride resistance. Mortars were produced with one ordinary Portland cement (OPC) as a reference and with four blended cements. The total porosity, the pore-size distribution and the porosity at the interfacial transition zone (ITZ) between aggregate and cement paste were analyzed and compared to the chloride resistance determined with a rapid migration test at three different ages (7, 28 and 182 days).

2 MATERIALS AND METHODS

2.1 *Materials*

An ordinary Portland cement (CEM I 42.5 according to EN 197-1) was used as reference. The second cement contained approximately 15 mass-% limestone powder (CEM II/A-LL). To produce the third cement, 15 mass-% of low-CaO fly ash were added in the laboratory to the second cement (CEM II/A-LL + V). The constituents of the fourth cement (CEM II/B-M (V-LL) correspond to the third one, but the blending already took place in the cement plant. This has the advantage that the sulfate carrier can be adjusted accordingly and the probability of incompatibilities between cement and superplasticizers are decreased. The fifth cement contained about 70 mass-% slag (CEM III/B). Cement composition is shown in Table 1. As aggregates for the mortars a quartz sand 0-2 mm was used (DIN EN 196-1). Water-to-cement ratio (w/c) of the reference mixture was 0.50. The other cements were dosed with identical volume and the amount of water was kept constant to keep the volume of paste constant as well (Table 2). Prisms (40 × 40 ×160 mm^3) and one plate (140 × 280 × 60 mm^3) were produced per cement type. At the age of 24 h the specimen were demolded and stored in water.

Type	CaO [%]	SiO_2 [%]	Al_2O_3 [%]	Fe_2O_3 [%]	MgO [%]	SO_3 [%]	Blaine [cm^2/g]	density [kg/m^3]
CEM I 42.5 N	62.3	19.9	4.8	2.8	1.8	3.0	3’012	3’130
CEM II/B-M (V-LL) 32.5 R	51.5	22.9	7.8	3.3	1.9	2.5	3’767	2’900
CEM II/A-LL 42.5 N	64.8	18.3	4.4	2.7	1.8	1.7	3’585	3’070
CEM III/B 42.5 N HS	50.4	30.4	9.5	1.2	5.6	0.8	4’230	3’000
Low CaO fly ash	6.4	55.1	28.4	7.2	1.6	0.0	-	2’290

Table 1: Composition and properties of cements and fly ash.

Cement type	w/c [volume]	w/c [mass]	Cement content [kg/m^3]	Water [kg/m^3]	Sand [kg/m^3]
CEM I	1.565	0.500	485	243	1’464
CEM II/A-LL	1.564	0.509	476	243	1’464
CEM II/B-M	1.566	0.540	449	243	1’464
CEM II/A-LL + V	1.564	0.536	385 + 68	243	1’464
CEM III/B	1.565	0.522	465	243	1’464

Table 2: Mix design of the mortars.

2.2 *Methods*

To measure mercury intrusion porosimetry (MIP) a mortar specimen per cement type was crushed, pieces without larger sand grains (< 1 mm) were selected (2.5-3.0 g) and freeze dried. MIP was measured with a pascal 140/440 (Themo Fisher Scientific Inc.) and the data were analyzed using the Washburn equation (Washburn, 1921).

Compressive strength was measure on three prisms per age according to European standard EN 196-1. Chloride resistance was determined with a rapid migration test according to Swiss standard SIA 262/1 on five cores (diameter = 50 mm, height = 50 mm) per mixture. A voltage of 20 V applied for 24 h accelerates chloride ingress into the water saturated samples. Afterwards, the samples are split and sprayed with an indicator solution to show the depth of the chloride front that is used to calculate the chloride migration coefficient D_m.

For the microstructural analysis, a 10-mm thick slice from the mid-section of a prism was cut perpendicular to its length axis, freeze dried, impregnated with epoxy resin, polished and carbon coated. Porosity was analysed with a Phillips ESEM-FEG XL30 with an acceleration voltage of 15 kV in the high vacuum mode according to the technique described in Leemann et al. (2006). Ten sand grains with a diameter > 1 mm were selected randomly. Above and below the sand grains eight images were made. The resolution of the images was 1600 x 2048 pixels with a pixel size of $0.12 \times 0.12\ \mu m^2$. Eighty images per mortar were analyzed with software developed in Matlab. Porosity was segmented and analyzed as a function of the distance to the aggregate.

3 RESULTS

3.1 Compressive strength

The blending of cement leads to a lower compressive strength at 7 and 28 days (Figure 1). However, after 182 days the differences are small. An exception is mortar CEM III/B, which displays a higher value than the other mortars. The relative strength development after 7 days depends on the mineral admixtures used. While mortar CEM II/A-LL shows the same behaviour as mortar CEM I, the compressive strength of the three mortars with either fly ash or slag increases more.

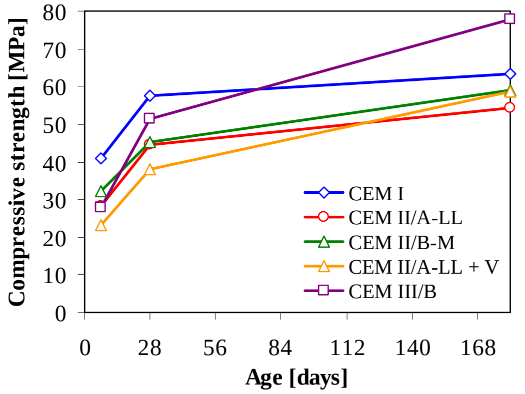

Figure 1: Compressive strength versus age.

3.2 Porosity

3.2.1 Mercury intrusion porosity

The total pore volume and the median of the pore size distribution decrease with age (Figures 2-4). At 7 days the pore volume of the mortars with blended cements is slightly higher than the on of the pure OPC (mortar CEM I). However, mortar CEM III/B shows the lowest median of the pore size distribution. At 28 days the pore volume of mortar CEM I and CEM III/B is smaller than the one of the other mortars (Figure 5). This applies as well for 182 days. Mortar CEM III/B shows the lowest median of the pore size distribution at 28 and 182 days, while the other mortars are very similar.

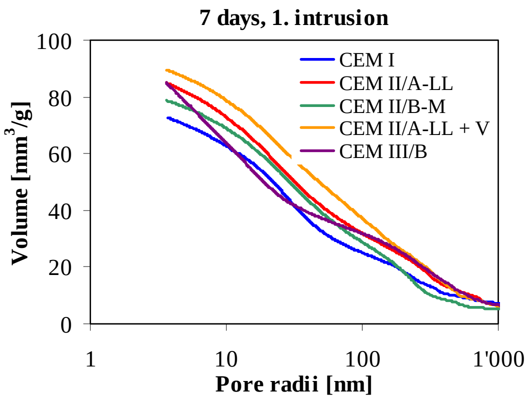

Figure 2: Total porosity and pore size distribution of mortar determined with MIP at an age of 7 days.

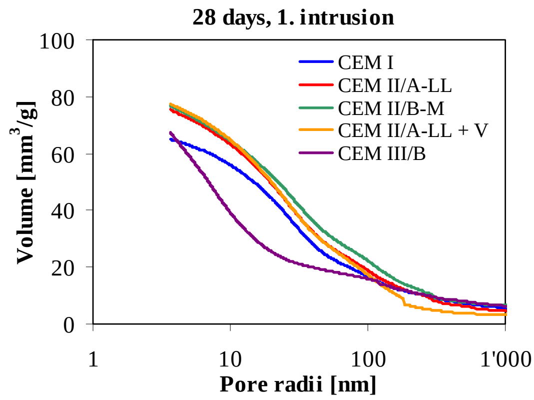

Figure 3: Total porosity and pore size distribution of mortar determined with MIP at an age of 28 days.

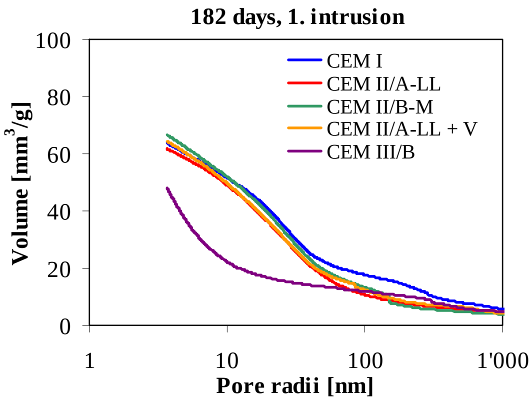

Figure 4: Total porosity and pore size distribution of mortar determined with MIP at an age of 1 days.

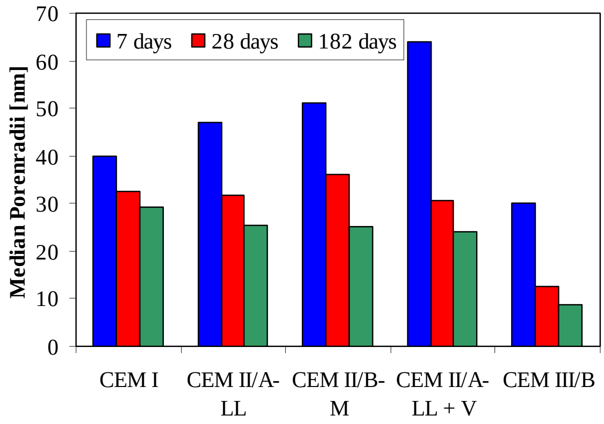

Figure 5: Median of the pore size distribution determined with MIP.

3.2.2 Interfacial transition zone (ITZ)

The pore volume in the ITZ shows the same pattern in all mortars; when the aggregates are approached, the pore volume starts to increase in a distance between 30 and 40 µm (Figure 6). There is a no change or even a decrease of the pore volume at a distance between 5-15 µm before a sudden increase in the pore volume occurs. The pore volume of mortar CEM II/A-LL+V starts to increase at a slightly greater distance to the aggregate than in the other mortars. But the differences between all mortars are relatively small.

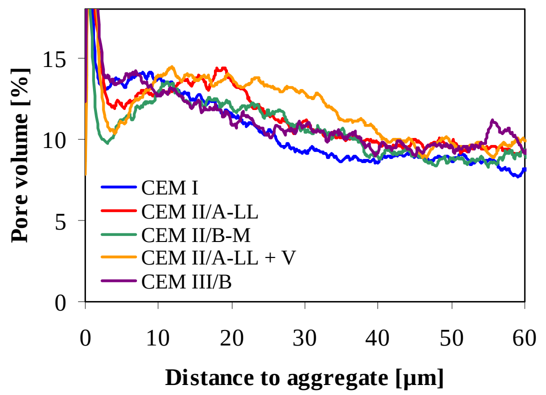

Figure 6: Pore volume in the different mortars as a function of the distance to the aggregates.

3.3 Chloride resistance

The chloride migration coefficient of all mortars decreases with age, which translates to an increasing chloride resistance (Figure 7). However, there are differences in its development with time. The decrease for mortar CEM I, CEM II/A-LL and CEM III/B from 28 to 182 days is only small, while the decrease for mortar CEM II/B-M and CEM II/A-LL+V are substantial.

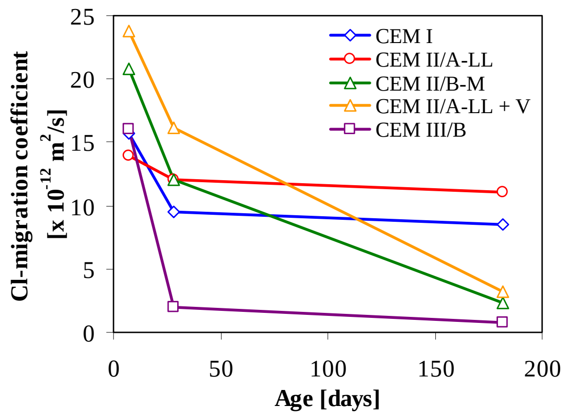

Figure 7: Chloride migration coefficient versus age.

4 DISCUSSION

Chloride migration coefficient decreases in an approximately linear way with increasing compressive strength (Figure 8). The only exception is mortar CEM III/B whose already very high chloride resistance does not decrease much between 28 and 182 day, despite a considerable strength gain. However, the relative increase of both compressive strength and chloride migration coefficient is higher for the mortars containing either fly ash or slag. This is a result of the relatively slow hydration kinetics of these two mineral admixtures. The absolute values for the chloride migration coefficient at 182 days are considerably lower than the ones for mortar CEM I and CEM II/A-LL. But as concrete is usually tested at an age of 28 days, when the chloride resistance of systems with fly ash or slag can still be lower, this beneficial effect may not be sufficiently taken into account by standards.

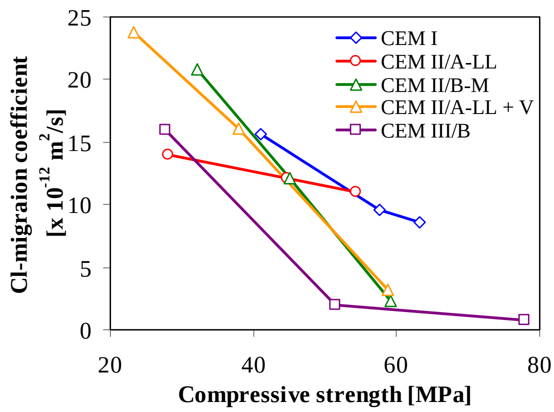

Figure 8: Chloride migration coefficient versus compressive strength.

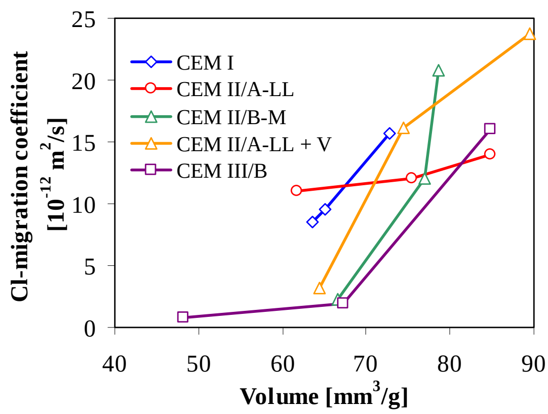

Figure 9: Chloride migration coefficient versus total porosity determined with MIP.

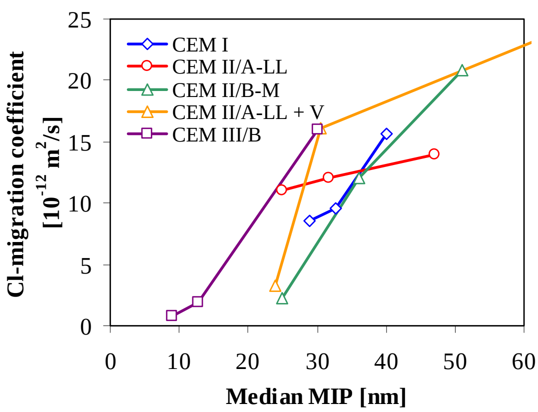

Figure 10: Chloride migration coefficient versus the median of the pore size distribution determined with MIP.

The total porosity and the median of the pore size distribution (Figures 9 and 10) show both a poor correlation with chloride migration coefficient, when all mortars are considered. However, if only one mortar produced with a specific cement is considered at different ages, a decrease of chloride migration coefficient goes together with a decrease of total porosity and a decrease of the median. There seems to be a cement-specific relation between porosity and chloride resistance. It must be pointed out that the determination of porosity in cementitious materials with MIP has some restrictions. The applied pressure during mercury intrusion may not be sufficient to fill very small pores. Therefore, the value for total porosity of samples with a relatively high amount of such small pores may be too small. Additionally, the measurements are significantly influenced by so-called “ink bottle pores”, larger pores that can only be filled through smaller pores (Diamond, 2000; Kaufmann et al., 2009). As a consequence, the resulting pore size distribution may overestimate the amount of small pores.

The increase of porosity approaching the aggregate is an effect of particle packing, the so-called wall effect (Farran, 1956), and bleeding (Leemann et al., 2010). The decrease of porosity at a distance from the aggregate between 5-15 µm is caused by the precipitation of portlandite (Leemann et al., 2010). The sharp increase in porosity just at the aggregate is an artefact of sample preparation due to cracks caused by drying shrinkage. However, the differences between the mortars are small. As the blending of cements has only a small impact on the interface between cement paste and aggregates, it can be expected that it also will have a small impact on the interface between cement paste and reinforcement bars. In addition, the blending of cements has no major influence on the pore volume in the ITZ.

5 CONCLUSIONS.

The effects of cement blending on chloride resistance and porosity of mortars have been studied.

The blending with 15 mass-% limestone powder in mortar CEM II/A-LL leads to slight decrease in compressive strength and chloride resistance compared to mortar CEM I (pure OPC). This type of cement seems to be especially suited for house building. However, if the blending of cement with 15 mass-% limestone powder is combined with a further blending with 15-mass-% fly ash, the resulting chloride resistance at 182 days is higher than the one of mortar CEM I at comparable compressive strength. Therefore, these types of cements are suited for structure with higher demands for durability. The best performance in regard to both compressive strength and chloride resistance is achieved by the use of slag in mortar CEM III/B.

The connection between porosity and permeability is not obvious in every case, because the characterisation of the pore systems is hindered by the limitations of the applied methods. However, it is clear that the excellent performance of mortar CEM III/B is due to high amount of fine pores and/or small pore necks. The similarity of the pore volume in the ITZ of the different mortars and their difference in chloride migration coefficient clearly indicates that the former has no major impact on permeability and chloride resistance.

6 ACKNOWLEDGEMENT

Pietro Lura is acknowledged for his critical review of the paper.

7 REFERENCES

Gartner, E. (2004) Industrially interesting approaches to “low-CO2” cements. *Cement and Concrete Research,* 34: 1489-1498.

Niu, Q, Feng, N, Yang, J, Zheng, X. (2002) Effect of superfine slag powder on cement properties. *Cement and Concrete Research,* 32: 615-621.

Luo, R, Cai, Y, Wang, C, Huang, X. (2003) Study of chloride binding and diffusion in GGBS concrete. *Cement and Concrete Research,* 33: 1-7.

Quellet, S, Bussière, B, Aubertin, M, Benzaazoua, M. (2007) Microstructural evolution of cemented paste backfill: mercury intrusion porosimetry test results. *Cement and Concrete Research,* 37: 1654-1665.

Loser, R, Lothenbach, B, Leemann, A, Tuchschmid, M. (2010) Chloride resistance of concrete and its binding capacity – comparison between experimental results and thermodynamic modeling. *Cement and Concrete Composites,* 32: 34-42.

Tsivilis, S, Chaniotakis, E, Batis, G, Meletiou, C, Kasselouri, V, Kakali, K. (1999) The effect of clinker and limestone quality on the gas permeability, water absorption and pore structure of limestone cement concrete. *Cement and Concrete Composites*, 21: 139-146.

Tsivilis, S, Tsantilas, J, Kakali, G, Chaniotakis, E, Sakellariou, A. (2003) The permeability of Portland limestone cement concrete. *Cement and Concrete Research*, 33: 1465-1471.

Matschei, T, Lothenbach, B, Glasser, FP. (2007) The role of calcium carbonate in cement hydration. *Cement and Concrete Research*, 37: 551-558.

Farran, J. (1956) Contribution mineralogique à l'étude de l'adherence entre les constituants hydrates des ciments et les materiaux enrobes. *Revue des Matériaux de Construction*, 490/491: 191–209.

Winslow, DN, Cohe,n MD, Bentz, DP, Snyder, KA, Garboczi, EJ. (1994) Percolation and pore structure in mortars and concrete. *Cement and Concrete Research*, 24: 25-37.

Garboczi, EJ, Bentz, DP. (1996) Modelling of the microstructure and transport properties of concrete. *Construction and Building Materials*, 10: 293-300.

Scrivener, KL, Nemati, KL. (1996) The percolation of pore space in the cement paste/aggregate interfacial zone of concrete. *Cement and Concrete Research*, 26: 35-40.

Scrivener, KL, Crumbie, AK, Pratt, PL. (1988) A study of the interfacial region between cement paste and aggregate in concrete. In: Mindess S, Sha SP, editors. Bonding in cementitious composites. Materials Research Society; 1988. 87-95.

Crumbie, AK. (1994) Ph.D thesis, University of London.

Diamond, S., Huang, J. (1998) The interfacial transition zone: reality or myth? In: Katz A., Bentur A., Alexander M., Arliguie G. (Eds.), The Interfacial Transition Zone in Cementitious Composites, E. and F.N. Spoon, London, 1-37.

Leemann, A, Münch, B, Gasser, P, Holzer, L. (2006) Influence of compaction on the interfacial transition zone and the permeability of concrete. *Cement and Concrete Research*, 36: 1425-1433.

Leemann, A, Loser, R, Münch, B. (2010) Influence of cement type on ITZ porosity and chloride resistance of self-compacting concrete. *Cement and Concrete Composites*, 32: 116-120.

Washburn, EW. (1921) Note on a Method of Determining the Distribution of Pore Sizes in a Porous Material. Proceedings of the National Academy of Sciences of the United States of America, 7, 115-116.

Diamond S. (2000) Mercury porosimetry: An inappropriate method for the measurement of pore size distributions in cement-based materials. *Cement and Concrete Research*, 30, 1517-1525.

Kaufmann, J, Loser, R, Leemann, A. (2009) Analysis of cement-bonded materials by multi-cycle mercury intrusion and nitrogen sorption. *Journal of Colloid and Interface Science*, 336: 730-737.